*Laser Physics, Vol. 12, No. 2, 2002, pp. 262–267.*




# Identification and Application of Quantum Trajectories in Above-Threshold Ionization

**G. G. Paulus[1], F. Grasbon[1], H. Walther[1], R. Kopold[2], and W. Becker[2]**

[1] *Max-Planck-Institute for Quantum Optics, Garching, 85748 Germany*
e-mail: ggp@mpq.mpg.de
[2] *Max-Born-Institute, Garching, 12489 Germany*

Received October 1, 2001

**Abstract**—We discuss two recent photoionization experiments with atoms in intense laser fields: First we study the dependence of photoelectron spectra on the intensity of the laser pulse. In a second experiment a photoelectron spectrum for elliptical polarization is discussed. With a quantum mechanical model the contribution of specific electron trajectories to the photoelectron spectra can be analyzed. In the presented cases, trajectories with long travel times are of significant importance. Despite of the distinctive quantum nature of the effects, some key features can be explained by classical electron trajectories.

## 1. INTRODUCTION

The interaction of atoms with intense laser fields can be investigated by analyzing the elementary processes: harmonic generation and photoionization. In the first case the production of harmonic photons of the incident laser field is studied. In the second case the two products of the ionization process—the photoelectrons and the ions—are detected and analyzed. Each of these three possible experiments shows a very distinctive effect; for reviews see [1–4]. For harmonic generation, the corresponding spectra, i.e., the harmonic yield as a function of the harmonic order/energy, starts with a steep decrease for the first few orders. Then it changes into a plateau-like extension of higher harmonics far into the soft X-ray spectral region. The plateau ends with a cutoff which depends linearly on the laser intensity. Due to the obvious potential for applications high harmonic generation (HHG) is subject of very detailed investigations.

Recent advances regarding photoionization open also in this field the door for applications: the measurement of attosecond pulses [5] and measurements regarding the so-called absolute phase of few-cycle pulses [6]. Above-threshold ionization (ATI) is photoionization with intense laser fields. The appearance of the envelope of the photoelectron spectra, i.e., the electron counts as a function of the kinetic energy of the electron, is quite similar to the harmonic spectrum described before: An ATI plateau (i.e., a photoelectron yield more or less independent of the energy) follows an initial steep drop for low photoelectron energies [7]. The cutoff energy of the ATI plateau again scales linearly with the intensity, but is much higher than in the case of HHG. If the energy resolution is high enough, a peak structure in the ATI spectra can be resolved. The energy positions $E_s$ of the peaks follow a generalized Einstein law

$$E_s = (n+s)\hbar\omega - |E_{IP}|$$

thus having a separation of the photon energy. Here $E_{IP}$ is the ionization potential of the atom, $\omega$ the laser (angular) frequency, $n$ the number of photons necessary to subdue the ionization threshold, and $s$ the number of photons absorbed in excess of those necessary for ionization.

For intense laser pulses ionization is a very fast process, possibly leading to complete ionization within the laser pulse (saturation). This on the one hand calls for short laser pulses and on the other hand for a high ionization threshold. With rare gas atoms and pulse durations of 50 fs the saturation intensity is in the range of $10^{14}$ W/cm$^2$. At such high intensities the quiver energy of a free electron, which by definition is the ponderomotive energy $U_P = \mathcal{E}^2/4\omega^2$ (atomic units) reaches considerable values, e.g., for $\lambda$ = 800 nm and $I$ = $10^{14}$ W/cm$^2$ we get $U_p$ = 6 eV which is more than the photon energy of 1.55 eV. The corresponding quiver amplitude of 8.4 Å is larger than the size of the atom itself. A photoelectron is a free electron and therefore it has to acquire the ponderomotive energy in addition to the ionization energy. Accordingly, the above equation has to be modified into

$$E_s = (n+s)\hbar\omega - |E_{IP}| - U_P. \qquad (1)$$

Equation (1) implies that for sufficiently high intensity $n$ photons are not anymore enough to ionize the atom, or in other words, the lowest order channel closes. For even higher intensities subsequent channels will close.

In order to study the influence of such a channel-closing on ATI, photoelectron spectra are studied in dependence on the intensity. In our experimental setup, small intensity intervals are possible due to the high repetition rate of the laser. Several channel-closing intensi-

ties are below the peak intensity of $I = 2 \times 10^{14}$ W/cm$^2$ of our laser system. We measured resonance-like effects at surprisingly high electron energies. Whole groups of peaks located in the ATI plateau region but well below the ATI cutoff shoot up at certain intensities.

A simple classical model can help to understand the fundamental processes during the interaction of the intense laser field with the atom [8–11]. The main idea is the classical treatment of the electron's trajectory, while it is driven by the electric field after being lifted into the continuum. Including the possibility to recombine or to rescatter at the ion core, the HHG and ATI cutoff energies can be calculated. In order to explain the complex influence of channel-closings in the plateau, however, an improved Keldysh type theoretical model was developed [12, 13]. The quantum mechanical approach can successfully reproduce the observed features and explain them via interference of many so-called "quantum orbits" of the electron. However, the classical model gives already a hint towards the interpretation.

The possibility, to analyze ATI spectra on the basis of quantum orbits, was also applied to an ATI spectrum for elliptical polarization. In this case quantum orbits could be identified that were responsible for specific energy intervals in the spectrum.

## 2. EXPERIMENTAL SETUP

Due to the fact that the electron count rates in the ATI plateau are two orders of magnitude lower than those for low-energy electrons, the prerequisite for studying features of the ATI plateau is a high laser pulse repetition rate. For our laser system it can be adjusted between 10 and 250 kHz. Owing to the flight-time of the photoelectrons, usually 100 kHz are chosen. The femtosecond pulses are created in a prism and chirped-mirror compensated Ti:$Al_2O_3$ oscillator. A modified commercial regenerative amplifier (Coherent RegA9050) pumped by an Argon ion laser increases the pulse energy up to 8 μJ. The second- and third-order dispersion introduced by the amplifier is balanced by a Proctor–Wise prism compressor and by chirped mirrors. We achieve pulse durations of 50 fs, the central wavelength is 800 nm. Intensities up to $2 \times 10^{14}$ W/cm$^2$ are obtained by focusing the laser beam with a specifically achromatized Fraunhofer lens to a diameter of 5 μm.

The electron spectrometer relies on the time-of-flight technique. Its doubly shielded flight distance is 450 mm long. Very fine nozzles with openings down to 5 μm are used to deliver the target gas into the interaction region. There the laser focus is placed tightly under the tip of the nozzle. This procedure has two advantages: Firstly, the gas pressure is relatively high mainly in the interaction region, and secondly, the effect of the integration of spectra originating from different regions of the focus and thus different intensities (volume effect) is reduced. The photoelectrons are registered by a micro-channel plate.

Due to the high repetition rate a 2 GHz multiscaler (FAST 7886) is used to measure the flight times and to record the data. This device, hosted by the computer that controls the experiment, is able to register a virtually arbitrary number of photoelectrons per laser shot without dead time. The resolution is 500 ps and, at high repetition rates, the transfer of the measured flight times to the computer memory is restricting the electron count rates to 200 kHz. The energy resolution at 30 eV is about 50 meV.

The intensity of the laser can be adjusted by either changing the focusing geometry, i.e., by changing the f-number of the achromat, or by a half-wave plate followed by a polarizer. The first possibility is employed for the coarse adjustment, while the latter is used for fine tuning. By mounting the half-wave plate on a stepper-driven rotary stage, it is possible to measure ATI spectra corresponding to different laser intensities without intervening. In fact, we scan a given intensity interval several times during the measurement of an intensity distribution of ATI spectra. This reduces the undesirable effects due to possible small drifts in the laser intensity.

The intensity distributions shown in this paper are taken with linear laser polarization and the polarization axis points into the direction of the electron detector. Spectra in an intensity interval of $(0.3–1.0)I_0$ in steps of $0.01I_0$ were recorded. $I_0$ is the maximum intensity for the respective measurement and depends on the focusing geometry. The small step size not only allows us precisely to follow the intensity dependence of the spectra, but also to produce animations. The latter proved to be of enormous help for identifying the interesting features reported in the first experiment. The second measurement is done with an ellipticity $\xi = 0.36$ of the incident light field and the electrons are detected in an angle of 30° with respect to the polarization axis.

## 3. CLASSICAL MODEL AND TRAJECTORY ANALYSIS

### *3.1. Classical Model*

The classical model subdivides the ionization process in several steps. In a first step, it is assumed that at a certain time $t_0$ the atom ionizes. This time determines the initial phase $\omega t_0$ of the linearly polarized laser field $\mathcal{E}(t) = \mathcal{E}_0 \sin \omega t$ when the electron is lifted into the continuum. In the second step, the electron trajectory is governed purely by the electric field. Due to the low photon energy (in relation to the ionization energy), the large excursion of the electron, and the high velocity the electron will attain, it is reasonable to choose $x(t_0) = 0$ and $\dot{x}(t_0) = 0$ as initial conditions for the trajectories. Depending on the initial phase $\omega t_0$ the electron may either leave the ion core direct or return to the vicinity of the core once ore several times. Upon its return—in a third step—three possibilities can be envisioned: If the electron recombines, UV photons are

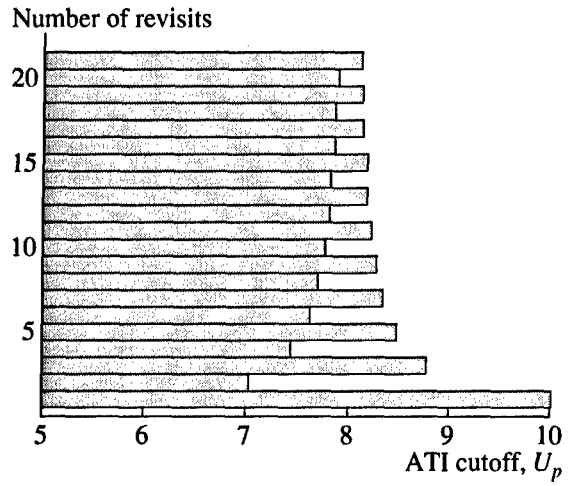


**Fig. 1.** ATI cutoff energies calculated with the classical model in dependence of the number of revisits. Only one pair of trajectories, namely that with the shortes travel time, is responsible for the highest energies.

generated (high harmonic generation); if it rescatters elastically, it may acquire additional energy from the field and leave the atom with high kinetic energy (Above-threshold ionization); and if it scatters inelastically, it may ionize the ion core, which leads to nonsequential double ionization. In the case of ATI the highest possible drift energy the electron can acquire after rescattering, can be easily calculated to $10U_p$, where $U_p$ is the ponderomotive drift energy, i.e., the quiver energy of a free electron in an oscillating electric field [11]. Hence, $10U_p$ corresponds to the cutoff energy of the ATI plateau given by the classical model in good agreement with the experiment.

Upon its return, however, the electron does not need to rescatter immediately at the ion core. Instead the electron can pass the core once or several times and rescatter at a later time. Figure 1 shows the maximum energy that the electron can acquire if it rescatters at the different revisits of the ion core. The maximum of $10U_p$ is only reached with rescattering at the first return, while higher-order returns lead to lower cutoff energies. The second-order return has the cutoff at $7U_p$, the third-order return at almost $9U_p$, and all higher-order returns are grouped around $8U_p$. The general features of the classical model will not be altered when some ellipticity is introduced to the laser field, because the trajectories of the electrons will be dominated by the big component of the electric field. Rescattering will be suppressed with increasing ellipticity and the maximum electron energy (cutoff energy) decreases for each order of revisit. However, the relative ordering of the cutoff energy with increasing return order will not be influenced. It should be noted that each final drift energy can be reached by a pair of trajectories. Only the cutoff energy relies on a single trajectory.

### *3.2. Quantum Orbit Analysis*

The idea of trajectories also appears in a quantum mechanical model that interprets the laser atom interaction in the spirit of Feynman's path integrals [13–15]. In order to gain more insight into the physical mechanism of ATI, the transition matrix element based on the Keldysh–Faisal–Reiss model [16] is written as an integral over all possible quantum paths leading to photoelectrons with momentum **p** that are allowed by energy conservation:

$$M_{\mathbf{p}} = \sum_n \delta(p^2/2 + U_P + |E_{IP}| - n\omega) \times \int dt \exp S_{\mathbf{p}}(t)/\hbar. \quad (2)$$

Here the phase $S$ is just the classical action along the electron trajectory (the "quantum orbit"), $\omega$ the laser frequency, $E_{IP}$ the ionization energy, and $U_p$ is again the ponderomotive energy. The integral can be approximated by the contributions of the saddle points determined by $\partial S/\partial t = 0$. For each electron energy a small number of stationary points contribute. This creates pairs (as in the classical model) of complex trajectories and the classical trajectories are resembled by the real part of these "quantum orbits." By comparing the exact numerical result with approximations that include only specific saddle points, the relevance of the saddle point and therefore its corresponding pair of quantum orbits can be determined. This technique of quantum orbit analysis provides unique access to ATI. In the next section an analysis is done for two cases, where especially the contribution of trajectories of higher order returns is of importance.

## 4. CHANNEL CLOSING

### *4.1. Experimental Results*

Figure 2a shows a few examples of ATI spectra which were measured while recording an intensity distribution as described above. It should be emphasized that no data processing has been carried out, in particular the counted electron numbers for an energy interval are given as measured. In general, the spectra behave as expected: As the intensity increases more electrons are counted. In addition, the ATI plateau develops. The maximum intensity $I_0$ can be calibrated by using the cutoff energy of $10U_p$. This leads to $I_0 \approx 8 \times 10^{13}$ W/cm$^2$. A closer look at the spectra reveals a striking difference between the spectra for $I \le 0.8I_0$ and those for higher intensity: Within a small intensity interval a group of ATI peaks corresponding to energies between about 15 and 25 eV grows very quickly. In the figure this is emphasized by horizontal lines drawn at the maximal heights of the plateaus. Increasing the intensity above $0.9I_0$ leads to a smaller growth rate of those peaks. The plateau, however, preserves its shape. For an interpretation, it should be kept in mind that a measured ATI spectrum is made up by contributions from all intensi-

ties $I \le I_0$ that are contained within the spatiotemporal pulse profile. This means that a spectrum for a fixed intensity would show the enhanced group of ATI peaks only at that intensity where it first appears in our measurement, namely at $I \approx 0.85I_0 = 7 \times 10^{13}$ W/cm$^2$. In other words, the enhancement happens at a well-defined intensity or at least within a very small intensity interval. Another feature of Fig. 2a is important: The apparent cutoff of the spectrum, defined to be slightly after the energy where the spectrum starts its final roll-off, makes a dramatic jump when the intensity rises from $0.8I_0$ to $0.9I_0$. The energy position of the corresponding cutoffs are marked with arrows.

A similar measurement is shown in Fig. 2b. Here, however, the intensity $I_0$ is higher. By evaluating the energy position of the ATI plateau cutoff as well as by comparing the spectra to those of Fig. 2a, $I_0$ is estimated to $1.4 \times 10^{14}$ W/cm$^2$. Owing to the higher maximum the enhancement described above now appears already at $0.45I_0$. Increasing the intensity leads to more and more electrons with high energy, while the appearance of the spectra qualitatively remains the same. At an intensity of $I \approx 0.85I_0 = 1.2 \times 10^{14}$ W/cm$^2$ again a group of ATI peaks begins to grow quickly within a very small intensity interval. This group of peaks is located at energies between about 25 and 40 eV and its height finally approaches the height of the group of ATI peaks described above.

Now, if one calculates the ponderomotive energies $U_p$ that correspond to the two intensities where the enhancements are observed, it turns out that these intensities are close to the 12- and 14-photon channel-closing. No effect of comparable clarity could be observed at the intensity corresponding to the 13-photon channel-closing.

### 4.2. *Trajectory Analysis*

The effects under investigation appear in the plateau region of the ATI spectra. Therefore, the Keldysh-ansatz has to be modified in order to include rescattering which is responsible for the plateau.

Figure 3a displays the spectrum calculated for the fixed intensity of the $n + s =: k = 12$ channel-closing and for one fixed intensity below and one above this value. One notices how a group of peaks rears up at the intensity of the channel-closing. Apart from the influence of the volume effect on the experimental data, this is very similar to what was described for Fig. 2. The same holds for higher intensities, the results of which are presented in Fig. 3b and 3c. Again there is a pronounced resonance-like behavior at the $k = 14$ channel-closing and almost nothing the like for the intensity corresponding to the $k = 13$ channel-closing. It should also be noticed that at the intensities of the channel-closings, the group of final peaks preceding the cutoff is suppressed. Hence, when the intensity increases

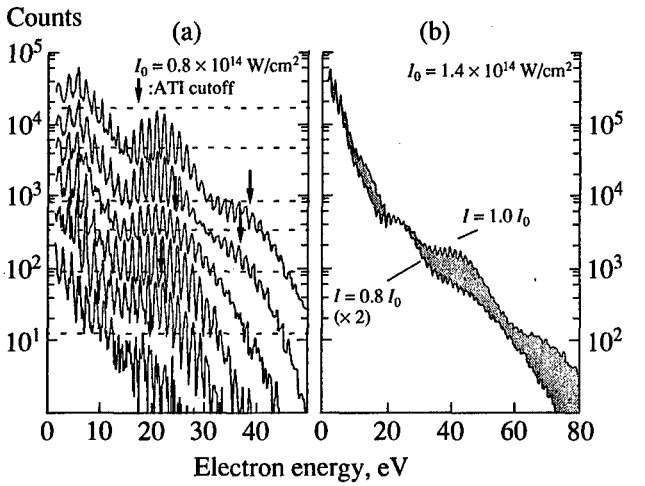


**Fig. 2.** (a) ATI spectra in argon at 800 nm recorded in the direction of the linearly polarized field for various intensities equally distributed between $0.5I_0$ and $1.0I_0$ with $I_0 \approx 8 \times 10^{13}$ W/cm$^2$. The horizontal lines mark the maxima of the plateaus for each intensity. The apparent cutoff positions of the spectra are indicated by arrows. (b) Measured ATI spectra for the same parameters as in Fig. 2a, but for $I_0 = 1.4 \times 10^{14}$ W/cm$^2$. The two traces are for $1.0I_0$ and $0.8I_0$, the counts in the latter case have been multiplied by a factor of 2.

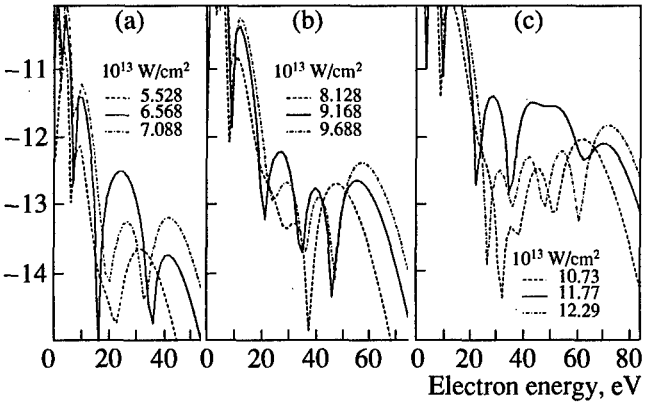


**Fig. 3.** Envelopes of ATI spectra below and above the intensities of the 12, 13, and 14-photon channel-closing as indicated in the panels. The calculation is based on the generalized Keldysh matrix element.

through the channel-closing, the apparent cutoff will experience the kind of jump observed in the data.

Having shown that the generalized Keldysh model is able to explain resonance-like features in the ATI plateau we would also like to give some explanations on their physical origins. Therefore, it should be possible to determine how many pairs of trajectories play a role under various conditions. Obviously, this can easily be done by comparing approximations using increasing numbers of trajectory pairs to the exact result. This has been done in Fig. 4 for the same conditions as in Fig. 3a. Figure 4a depicts the situation for an intensity

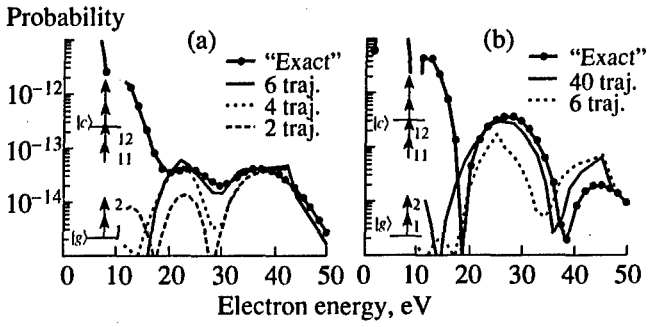


**Fig. 4.** Approximation of the "exact" result (cf. Fig. 3a) by contributions of various numbers of quantum trajectories. In (a) the intensity is lower than the $k = 12$ channel-closing intensity ($I = 6.05 \times 10^{13}$ W/cm$^2$) and only 3 pairs of trajectories give an excellent agreement with the "exact" calculation. At the channel-closing intensity ($I = 6.57 \times 10^{13}$ W/cm$^2$) much more trajectories are necessary (b). Note that only rescattering orbits are included. Therefore the approximations do not work for energies below 20 eV.

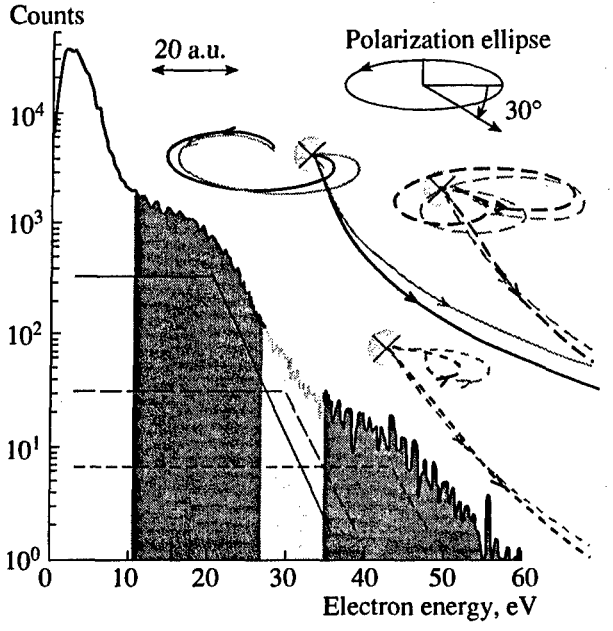


**Fig. 5.** ATI spectrum in xenon at 800 nm for an elliptically polarized laser field with ellipticity $\xi = 0.36$ and intensity $7.7 \times 10^{13}$ W/cm$^2$ for emission at an angle with respect to the polarization axis as indicated. The different steps of the spectrum are shaded in gray. For each step, the responsible calculated quantum orbits are displayed. The crosses mark the position of the atom, and the length scale of the orbits is given in the upper left of the figure.

just below the $k = 12$ channel-closing. A few pairs of trajectories are sufficient to give an excellent approximation of the exact result. This is very different at the channel-closing intensity. A large number of trajectories is necessary to come close to the exact solution. It is also interesting to see that the modulus of the amplitude of the individual pairs is similar at and off the channel-closing intensity. The difference is that for channel-closing all trajectories interfere constructively while they interfere in a random way otherwise. Now, the open question is, why do the trajectories interfere constructively just at the channel-closing intensities. While we cannot answer this another point seems worth mentioning: The resonance-like behavior is restricted to the lower electron energies in the ATI plateau and the last hump is not affected (actually, the last hump is suppressed a little bit). This can easily be understood by recalling the classical model and the dependence of the classical cutoff energy on the return order (see Fig. 1). For the highest electron energies there is simply only one pair of trajectories available which could interfere constructively. However, in the low-energetic part of the plateau all types of trajectories can contribute to the electron count rate.

It should be noted that a similar, if not the same, effect has already been explained in a different way [17, 18]. There, multi-photon resonances with Rydberg states were made responsible for the enhancements. Accordingly, it was predicted that the Rydberg series will be mapped onto the ATI spectra [19]. Although experiments with pulses three times longer than ours show some fine structure in the plateau region, there is no definite agreement with theory [20]. The mere existence of fine structure should not be taken as proof of bound states being involved. Interference structures in the ATI spectra together with spatiotemporal averaging in the focus also lead to structured ATI peaks under suitable conditions. This has been shown by simulating the spatiotemporal averaging with a Keldysh-type theory [21]. A more stringent test is whether the well-known resonances for low energy electrons [19] appear at exactly the same intensities than the structures at high electron energy.

The calculations in [17, 18], were done for long-pulse conditions. It is noteworthy that the difference in pulse length appears to have such important consequences. For our conditions, i.e., such short pulses that Rydberg states are hard to resolve [22], it can be shown experimentally that atomic resonances are not involved: The Freeman resonances of the two bound states that we are able to resolve more or less (probably $4f$ and $5f$) appear at other intensities than the enhancements in the plateau.

## 5. ATI FOR ELLIPTICALLY POLARIZED LIGHT

Another experimental demonstration of the role of quantum orbits to the shape of an ATI-spectrum is achieved for the case that the incident light is elliptically polarized. This condition makes the contribution of different quantum orbits in the ATI spectrum easily distinguishable, since their strength and their corresponding energetic parts in the spectrum are different [23].

In the ATI spectrum of Fig. 5 a staircase with several steps is observed for elliptical polarization. The rich structure of the spectrum is predicted by the quantum

orbit approximation based on Eq. (2). The scheme of these theoretical predictions is represented by the straight lines, representing the calculated plateau behavior for each type of quantum orbit. The top step in the spectrum does not concern us here: it is made up by the "direct" electrons, that do not rescatter. For the remaining steps, each can be attributed to the particular pairs of quantum orbits identified in the figure. The orbits differ in the number of passing by the ion core before rescattering. The physical origin of the steps is as follows: in the process of tunneling, the electron most likely starts its orbit with zero velocity after tunneling. For elliptical polarization, however, in order that such an orbit returns to the parent ion, its starting velocity must be non-zero. The larger it is, the smaller the contribution of the associated orbit. Such is the case for the shortest orbits, which require a particularly large starting velocity. Since these electrons can reach, as already predicted by the classical model, the highest kinetic energies, they contribute alone to the high energetic part of the spectrum. Orbits that pass the core once need a much smaller starting velocity and therefore are much more probable. However, the maximal possible energy for this class of orbits is much smaller (cf. Fig. 1). Therefore these orbits give the main contribution to the low energetic part of the ATI plateau. Theory also predicts a small step in between the two main ones; the experimental data show an indication of that.

## 6. CONCLUSION

We discussed new experimental and theoretical results of ATI spectra, in particular for the ATI plateau region. Firstly, resonance-like features in the intensity dependence of high-order ATI peaks were found to originate from channel-closings. The decomposition of the ATI matrix element into the relevant quantum trajectories let us to the conclusion that the enhancements of groups of ATI peaks in the plateau is caused by constructive interference of many trajectories at channel-closings. Between channel-closings the interference of the trajectories is random with the consequence that the strongest pairs of trajectories (i.e., those with the shortest travel times) are sufficient to calculate the corresponding spectrum. Details of the ATI spectra, like the energy position of the enhancements can be explained. Secondly, we showed that an ATI spectrum could be decomposed in energetic regions of the spectrum that are caused by single fundamental pairs of quantum orbits. This was made possible again with the help of the same theoretical approach.

## REFERENCES


1. DiMauro, L.F. and Agostini, P., 1995, *Adv. At., Mol., Opt. Phys.*, **35**, 79.
2. L'Huillier, A., Antoine, Ph., and Lewenstein, M., 1999, *Adv. At., Mol., Opt. Phys.*, **41**, 83.
3. Joachain, C.J., Doerr, M., and Kylstra, N.J., 2000, *Adv. At., Mol., Opt. Phys.*, **42**, 225.
4. Brabec, Th. and Krausz, F., 2000, *Rev. Mod. Phys.*, **72**, 545.
5. Paul, P.M., Toma, E.S., Berger, P., Mullot, G., Auge, F., Balcou, Ph., Muller, H.G., and Agostini, P., 2001, *Science*, **292**, 1689.
6. Paulus, G.G., Grasbon, F., Walther, H., Villoresi, P., Nisoli, M., Stagira, S., Priori, E., and De Silvestri, S., *Nature* (in press).
7. Paulus, G.G., Nicklich, W., Xu Huale, Lambropoulos, P., and Walther, H., 1994, *Phys. Rev. Lett.*, **72**, 2851.
8. van Linden van den Heuvell, H.B. and Muller, H.G., 1988, *Multiphoton Processes, Studies in Modern Optics* (Cambridge), no. 8, p. 25.
9. Corkum, P.B., Burnett, N.H., and Brunel, F., 1989, *Phys. Rev. Lett.*, **62**, 1259.
10. Corkum, P.B., 1993, *Phys. Rev. Lett.*, **71**, 1994.
11. Paulus, G.G., Becker, W., Nicklich, W., and Walther, H., 1994, *J. Phys. B*, **27**, L703.
12. Lohr, A., Kleber, M., Kopold, R., and Becker, W., 1997, *Phys. Rev. A*, **55**, R4003.
13. Kopold, R., Becker, W., and Kleber, M., 2000, *Opt. Commun.*, **179**, 39.
14. Lewenstein, M., Kulander, K.C., Schafer, K.J., and Bucksbaum, P.H., 1995, *Phys. Rev. A*, **51**, 1495.
15. Kopold, R., Milosevic, D.B., and Becker, W., 2000, *Phys. Rev. Lett.*, **84**, 3831.
16. Keldysh, L.V., 1964, *Zh. Eksp. Teor. Fiz.*, **47**, 1945 [1965, *Sov. Phys. JETP*, **20**, 1307]; Faisal, F.H.M., 1973, *J. Phys. B*, **6**, L89; Reiss, H.R., 1980, *Phys. Rev. A*, **22**, 1786.
17. Muller, H.G. and Kooiman, F.C., 1998, *Phys. Rev. Lett.*, **81**, 1207.
18. Muller, H.G., 1999, *Phys. Rev. Lett.*, **83**, 3158.
19. This is reminiscent of the so-called Freeman resonances (Freeman, R.R., Bucksbaum, P.H., Milchberg, H., Darack, S., Schumacher, D., and Geusic, M.E., 1987, *Phys. Rev. Lett.*, **59**, 1092). However, they are expected to be restricted to low electron energies (1 to $3\hbar\omega$).
20. See Fig. 4. in Nandor, M., Walker, M.A., Van Woerkom, L.D., and Muller, H.G., 1999, *Phys. Rev. A*, **60**, R1771.
21. Kopold, R., Becker, W., Kleber, M., and Paulus G.G., *J. Phys. B* (submitted).
22. The lowest excited state that plays a role is the 4*f* state. Its Kepler time is roughly 10 fs long. This has to be compared to the pulse duration of 50 fs (FWHM). Assuming a $\mathrm{sech}^2$ pulse shape, the intensity in a 10 fs interval around the pulse maximum changes by 3%, for a 20 fs interval by 12%. Therefore, for a peak intensity of $0.7 \times 10^{14}$ W/cm$^2$, the exited states are shifted by approximately 0.5 eV within two Kepler revolutions of a 4f electron. If we assume that at least two revolutions are necessary in order to build up a resonance enhancement, this leads to a contradiction because within this time the states are shifted stronger than the level spacing. Besides that, it is not clear whether the concept of the ponderomotive shift of the excited states can be applied for single optical cycles or even fractions of them.
23. Salières, P., Carré, B., Le Déroff, L., Grasbon, F., Paulus, G.G., Walther, H., Kopold, R., Becker, W., Milošević, D.B., Sanpera, A., and Lewenstein, M., 2001, *Science*, **292**, 902.